DINAME 2023 - Proceedings of the XIX International Symposium on Dynamic Problems of Mechanics,
A.S. De Paula, A.T. Fabro and M.R. Machado (Editors), ABCM.
Pirenópolis, Go, Brazil, February 26th to March 3rd, 2023

Modeling and control for Vector-P UAV

Clécio Fischer[1], Éder Alves Moura[2], Leonardo Murilo Nepomuceno[3], Roberto Gil Annes da Silva[3] and Luiz Carlos Sandoval Góes[3]

[1] Department of Mechanical Engineering, Aeronautics Institute of Technology, São José dos Campos, Brazil

Federal Institute of Education, Science and Technology of São Paulo, São José dos Campos, Brazil

[2] Department of Mechanical Engineering, Aeronautics Institute of Technology, São José dos Campos, Brazil

Department of Electrical Engineering, Federal University of Uberlandia, Uberlândia, Brazil

[3] Department of Mechanical Engineering, Aeronautics Institute of Technology, São José dos Campos, Brazil

Abstract: This work proposes a Autopilot with Stability Augmentation System (SAS) capabitilities to control the Vector-P fixed-wing aircraft, which is an Unmanned Aerial Vehicle (UAV) manufactured by Intellitech Microsystems and designed to install avionics and data acquisition systems. This aircraft will be destined to fulfill flight missions that can be remotely piloted or through autonomous flights. An output feedback Linear Quadratic Regulator (LQR) is designed to accomplish the Autopilot/SAS task. The SAS is proposed to modify the open-loop natural response for the longitudinal and latero-directional flight qualities, and the Autopilot/SAS aims to maintain straight-and-level flight with zero sideslip. An identified dynamical model of the Vector-P was adopted for the LQR design. The LQR was manually tuned and the gains provide a well-performing automatic controller to keep track of speed, attitude and altitude references; where the open-loop and closed-loop simulation, for the complete dynamics of the aircraft, are shown. The results show that the proposed control system achieved the objectives of improving flight characteristics, which will facilitate the fulfillment of flight missions.

Keywords: lqr, output-feedback controller, stability augmentation system, autopilot, uav.

INTRODUCTION

The growing adoption of Unmanned Aerial Vehicle (UAV) in recent years is demanding the use of advanced engineering tools for their design to decrease production and use costs and increase safety standards, as their applications are increasingly broader and by an increasingly less specialized public. Additionally, the popularization of several low-cost and easily accessible on-board flight controllers and sensors, due to advances in microelectronics, have allowed academic research to test theories and methods in practice, which was previously only possible with manned aircraft or larger and more expensive equipment. This work makes use of the aircraft Vector-P, a UAV shown in Fig. 1 that is manufactured by Intellitech Microsystems and its configuration is designed to install custom avionics and data acquisition systems. Vector-P has a pusher engine to avoid vibration interference in the sensors installed near of the nose of the aircraft. This UAV is a fixed-wing vehicle built with composite material. The Vector-P had their electronic systems integrated and operated in the Aeronautical System Lab (LSA) at the Aeronautics Institute of Technology (ITA-Brazil). This radio-controlled platform is intended to be used for study purposes, such as the analysis of different devices for flight test data acquisition and the evaluation of different systems identification methods.

As a study platform, Vector-P was the object of several analyzes in the LSA, having the models of longitudinal and latero-directional dynamics identified. The identification procedure aims to obtain the parameters for a mathematical model of a system, e.g. an aeroelastic system Barbosa *et al.* (2019). The identification of longitudinal and latero-directional dynamic models has already been applied to Vector-P. In this work the identified models will be used for the design of an automatic flight control, which consists of an Autopilot with additional features of a Stability Augmentation System (SAS), so that the Vector-P has the autonomy to maintain straight-and-level flight with zero sideslip and modify the aircraft open-loop dynamic characteristics. Also, throughout the various studies that this aircraft underwent at LSA, the need to design a control system for the Autopilot/SAS functions was identified, with the aim of improving its flight characteristics. The Autopilot/SAS system aims to control the aircraft's attitude, altitude and speed as much as to modify the natural response of the longitudinal and latero-directional dynamics. To this end its proposed a configuration of two simultaneous controllers, one for the longitudinal dynamics and other for the latero-directional dynamics, using an output-feedback Linear Quadratic Regulator (LQR) with and manual adjustment of the tuned parameters.

The LQR is a model-based control algorithm used to stabilize and maintain the desired performance of a system by adjusting the control inputs. In the output feedback variation of LQR, the control inputs are based on a limited set of measurements of the system (outputs), rather than the full state vector. This type of LQR is particularly useful when the state of the system is not easily measurable, as in this case.

Thus, the tuning process of the LQR controllers for the UAV Vector-P, with output-feedback restriction and using an

Figure 1: Vector-P.

identified model, will be presented in this work, by presenting the adopted modeling for the dynamics, in addition to the parameters found in the identification process, detailing the design of the control system and showing the results obtained with the control system actuation, through simulations.

MODELING AND IDENTIFICATION OF VECTOR-P DYNAMICS

This section presents the modeling of the flight dynamics and identified parameters of the UAV and the simplifications adopted for the longitudinal and latero-additional movement. Figure 2 presents the adopted relations for the reference axis, where: $\mathscr{F}_B = \{Xb, Yb, Zb\}$ is the body-fixed axis; $\mathscr{F}_s = \{Xs, Ys, Zs\}$ is the stability axis; $\mathscr{F}_w = \{Xw, Yw, Zw\}$ as the wind axis; and $\mathscr{F}_R = \{Xr, Yr, Zr\}$ is the ground reference axis, fixed at the start position and initially aligned with $\mathscr{F}_B$. All the frames relative to the aircraft (excluding $\mathscr{F}_R$) are centered to the aircraft center of mass (CG).

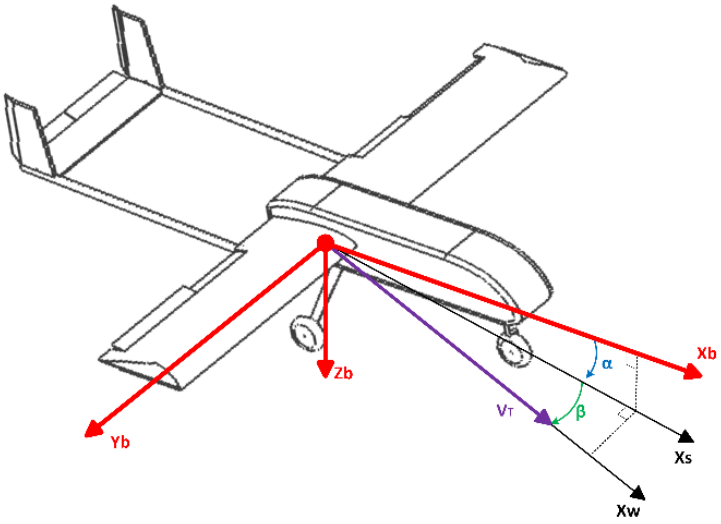

Figure 2: Description of the coordinate systems adopted in the modeling for the design of the control system.

The flat-earth body-axes differential equation of motion that describes the behavior of an aircraft can be found in references such as Stevens and Lewis (1992), Nelson (1989) and Etkin and Reid (1995), for the state space equation:

$$\dot{\mathbf{x}} = \mathbf{f}(\mathbf{x}, \mathbf{u}), \tag{1}$$

where the state vector and the control input vector are defined by:

$$\mathbf{x} = [V\ \alpha\ q\ \theta\ h\ x\ \beta\ \phi\ p\ r\ \psi\ y]^{\mathrm{T}} \in \mathbb{R}^{12}, \text{ and} \tag{2}$$

$$\mathbf{u} = [\delta_t\ \delta_e\ \delta_a\ \delta_r]^{\mathrm{T}} \in \mathbb{R}^4, \tag{3}$$

for which, we define that: $\Phi = [\phi\ \theta\ \psi]^{\mathrm{T}} \in \mathbb{R}^3$ represents the aircraft attitude, given by the relation of $\mathscr{F}_B$ with respect to $\mathscr{F}_R$; $\omega = [p\ q\ r]^{\mathrm{T}} \in \mathbb{R}^3$ is the angular velocity in $\mathscr{F}_B$; $\mathbf{r} = [x\ y\ z]^{\mathrm{T}} \in \mathbb{R}^3$ is the aircraft relative position, represented by the vector that conects the origin of $\mathscr{F}_R$ to $\mathscr{F}_B$ and expressed in $\mathscr{F}_R$ — an additional definition is the aircraft's altitude, given by $h = -z$; V is the aircraft true velocity; and α and β are the aerodynamic angles and represents, respectively, the attitude from $\mathscr{F}_W$ with respect to $\mathscr{F}_S$ and from $\mathscr{F}_S$ to body axes $\mathscr{F}_B$. The control inputs shown in Eq. 3 are, respectively, the throttle deflection, in percentage, and the deflections of the elevator, the aileron and the rudder, in degrees.

The structural characteristics of Vector-P are shown in Tab. 1.

Table 1: Manufacturer's data of the VECTOR-P airplane

Variable	Value	Variable	Simbol	Value
Wingspan	2.6 m	Mass	m	31.5 kg
Fuselage Length	1.525 m	Wing area	S	1.15m²
Engine	7.5 hp 2-stroke	Chord	c	0.445m
Cruise Speed	35.8 m/s	Span	b	2.58m
Max Altitude	3000 m	Inertia	I_{xx}	3.14 kg m²
Empty weight	19.7 kg	Inertia	I_{yy}	8.25 kg m²
Max Takeoff Weight	34 kg	Inertia	I_{zz}	10.40 kg m²
		Inertia	I_{xz}	0.01 kg m²

The equations adopted to describe the P-Vector dynamics are presented from Eq. 4 to Eq.11. the derivatives of stability associated with these equations are shown in Tab. 2 and these parameters were obtained from the identified longitudinal model presented in Santos (2013) and from the latero-directional model presented in Fischer *et al.* (2018).

$$C_X = -C_D\ cos(\alpha) + C_L sin(\alpha), \tag{4}$$

$$C_Y = C_{y\beta}\beta + C_{y\delta_a}\delta_a + C_{y\delta_r}\delta_r + (C_{yp}p + C_{yr}r)\frac{b}{V_t}, \tag{5}$$

$$C_Z = -C_{D_0}\ sin(\alpha) + C_L cos(\alpha), \tag{6}$$

$$C_D = C_{D_0} + \frac{1}{\pi eAR}C_L^2, \tag{7}$$

$$C_L = C_{L_0} + C_{L\alpha}\alpha + C_{L\delta_e}\delta_e + C_{Lq}q\frac{\bar{c}}{V_t}, \tag{8}$$

$$C_l = C_{l\beta}\beta + C_{l\delta_a}\delta_a + C_{l\delta_r}\delta_r + (C_{lp}p + C_{lr}r)\frac{b}{V_t}, \tag{9}$$

$$C_m = C_{m_0} + C_{m\alpha}\alpha + C_{m\delta_e}\delta_e + C_{mq}q\frac{\bar{c}}{V_t}, \text{ and} \tag{10}$$

$$C_n = C_{n\beta}\beta + C_{n\delta_a}\delta_a + C_{n\delta_r}\delta_r + (C_{np}p + C_{nr}r)\frac{b}{V_t}. \tag{11}$$

Table 2: Identified parameters and CR

Longitudinal Parameter	C_{L_0}	C_{L_α}	C_{L_de}	C_{L_q}	C_{D_0}	C_{m_0}	C_{m_α}	C_{m_de}	C_{m_q}
Value	0.524	3.388	0.957	2.1878	0.049	-0.085	-0.551	-0.999	-15.719
Latero-directional Parameter	C_{y_β}	$C_{y\delta_a}$	$C_{y\delta_r}$	C_{y_p}	C_{y_r}	C_{l_β}	$C_{l\delta_a}$	$C_{l\delta_r}$	C_{l_p}
Value	0.0290	0.0176	-0.0082	-0.0243	0.0202	-0.0285	0.0666	-0.0113	-0.1317
Latero-directional Parameter	C_{l_r}	C_{n_β}	$C_{n\delta_a}$	$C_{n\delta_r}$	C_{n_p}	C_{n_r}			
Value	0.0490	0.0900	0.0224	0.0425	-0.0772	-0.1627			

AUTOPILOT/SAS CONTROL SYSTEM DESIGN

Considering the set of equations that describing the Vector-P flight dynamics, Eq. (1-11), the structural parameters presented in Tab. 1 and the identified parameters of the stability derivatives shown in Tab. 2, the objective is to design a feedback control system for the longitudinal and latero-directional stabilization. To this end, is adopted the strategy of separete the longitudinal from the latero-directional controls and, for each one, an LQR is tuned over and equilibrium point. This proposition is schematized in Fig. 3, where $\mathbf{u}_{eq}$ is numerically computed to achieve the desired values of $\mathbf{x}_{eq}$ (Stevens and Lewis, 1992; Nelson, 1989), which represents the desired flight condition.

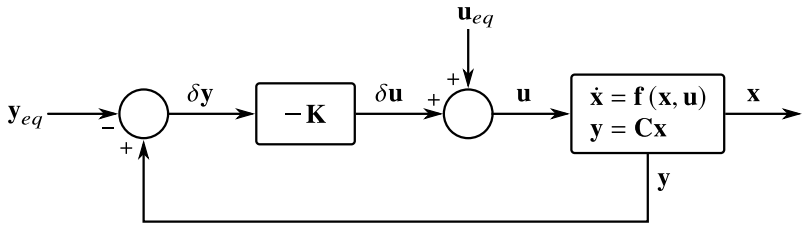

Figure 3: Schematic view of the LQR system to control system in $\mathbf{x}_{eq}$ and $\mathbf{u}_{eq}$.

The first step for the design of a LQR controller to a nonlinear system is to obtain a linearized version of the dynamic equation. Therefore, as it is adopted the feedback outpout, a restrict set of state variables is measured, and it is given by:

$$\mathbf{y} = \mathbf{C}\mathbf{x}. \tag{12}$$

The linearization is carried out assuming small perturbations over some equilibrium operation point $(\mathbf{x}_{eq}, \mathbf{u}_{eq})$ and the linear state equation is defined here by:

$$\delta\dot{\mathbf{x}} = \mathbf{A}\delta\mathbf{x} + \mathbf{B}\mathbf{u}, \tag{13}$$

where $\delta\mathbf{y} = \mathbf{y} - \mathbf{y}_{eq} = \mathbf{C}\delta x$ is the error of control objectives; $\delta\mathbf{x} = \mathbf{x} - \mathbf{x}_{eq}$ and $\mathbf{u} = \mathbf{u}_{eq} + \delta\mathbf{u}$; $\delta\mathbf{x}$ and $\delta\mathbf{u}$ are, respectively, the state and input control deviation from $\mathbf{x}_{eq}$ and $\mathbf{u}_{eq}$, in Eq. (1); and $\mathbf{y}_{eq} = \mathbf{C}\mathbf{x}_{eq}$. The matrices $\mathbf{A}$ and $\mathbf{B}$ are defined as follows:

$$\mathbf{A} = \frac{\partial \mathbf{f}(\mathbf{x},\mathbf{u})}{\partial \mathbf{x}}, \text{ and} \tag{14}$$

$$\mathbf{B} = \frac{\partial \mathbf{f}(\mathbf{x},\mathbf{u})}{\partial \mathbf{u}}. \tag{15}$$

For the linearized system expressed by Eq. (13) and the feedback configuration presented in Fig. 3, the LQR determines the gain matrix $\mathbf{K}$, for the control input variation $\delta\mathbf{u} = -\mathbf{K}\delta\mathbf{y}$, that minimizes the quadratic cost:

$$J(\delta\mathbf{u}) = \int_0^\infty \left(\delta\mathbf{x}^{\mathrm{T}}\mathbf{Q}\delta\mathbf{x} + \delta\mathbf{u}^{\mathrm{T}}\mathbf{R}\delta\mathbf{u}\right)dt, \tag{16}$$

given an initial condition $\delta\mathbf{y}(0)$, the tuning matrices $\mathbf{Q}$ and $\mathbf{R}$ (those matrices are, respectively, positive semidefinite and positive definite), and the controllable pair $(\mathbf{A},\mathbf{B})$. Thus, it is possible to compute the feedback gain matrix by: $\mathbf{K} = \mathbf{R}^{-1}\mathbf{B}^{\mathrm{T}}\mathbf{P}$, where the matrix $\mathbf{P}$ is the solution of the Algebraic Riccati Equation (ARE):

$$\mathbf{A}^{\mathrm{T}}\mathbf{P} + \mathbf{P}\mathbf{A} - \mathbf{P}\mathbf{B}\mathbf{R}^{-1}\mathbf{B}^{\mathrm{T}} + \mathbf{Q} = \mathbf{0}. \tag{17}$$

As established, this system has the separation of longitudinal and latero-directional controls, which implies that two feedback systems need to be designed. In this way, the state vector is divided into two parts: $\mathbf{x}_{lo} = [V\ \alpha\ q\ \theta\ h\ x]^{\mathrm{T}} \in \mathbb{R}^6$, related to the aircraft longitudinal dynamics, and $\mathbf{x}_{ld} = [\beta\ \phi\ p\ r\ \psi\ y]^{\mathrm{T}} \in \mathbb{R}^6$, related to the aircraft latero-directional dynamics. Likewise, the same separation is valid to $\mathbf{x}_{eq}$ and $\mathbf{u}_{eq}$. It is adopted the measurement vectors $\mathbf{y}_{lo} = [V\ \alpha\ q\ \theta\ h]^{\mathrm{T}} \in \mathbb{R}^5$ and $\mathbf{y}_{ld} = [\phi\ p\ r\ \psi]^{\mathrm{T}} \in \mathbb{R}^4$, which defines, respectively, the measurement matrices:

$$\mathbf{C}_{lo} = \begin{bmatrix} 1 & 0 & 0 & 0 & 0 & 0 \\ 0 & 1 & 0 & 0 & 0 & 0 \\ 0 & 0 & 1 & 0 & 0 & 0 \\ 0 & 0 & 0 & 1 & 0 & 0 \\ 0 & 0 & 0 & 0 & 1 & 0 \end{bmatrix} \in \mathbb{R}^{5\times 6}, \text{ and} \tag{18}$$

$$\mathbf{C}_{ld} = \begin{bmatrix} 0 & 1 & 0 & 0 & 0 & 0 \\ 0 & 0 & 1 & 0 & 0 & 0 \\ 0 & 0 & 0 & 1 & 0 & 0 \\ 0 & 0 & 0 & 0 & 1 & 0 \end{bmatrix} \in \mathbb{R}^{4\times 6}. \tag{19}$$

The closed-loop dynamics for the linearized system is described by:

$$\delta\dot{\mathbf{x}} = (\mathbf{A} - \mathbf{BKC})\,\delta\mathbf{x} + \mathbf{B}\mathbf{u}_{eq}. \tag{20}$$

Analysis of open-loop flight condition

Defining a desired flight condition $\mathbf{x}_{eq}$ and given the complete nonlinear model of the Vector-P dynamics, a numerical search was performed to find the control inputs $\mathbf{u}_{eq}$ that keeps the aircraft at equilibrium position. The numerical search was implemented with the Matlab algorithm `fsolve`. The set of constraints applied to the state variables and the found equilibrium control input are shown in Tab. 3.

Table 3: Flight condition.

$\mathbf{x}_{eq}$ constraint	V	α	θ	h	p	q	r
Value	33 m/s	-0.24 deg	-0.24 deg	680 m	0 m/s	0 m/s	0 m/s
$\mathbf{u}_{eq}$	δ_t	δ_e	δ_a	δ_r			
Value	32.82%	-4.7409 deg	0 deg	0 deg			

Given the values of $\mathbf{x}_{eq}$ and $\mathbf{u}_{eq}$ and the Eq. (1), the linearized system can be obtained by applying the Eq. (14) and the Eq. (15). As a result, the dynamical modes of Vector-P are presented in Tab. 4, and its representation is shown in Fig. 4, where the longitudinal and latero-directional modes are highlithed. Also, the matrices $\mathbf{A}$ and $\mathbf{B}$, for both situations, are presented in Tab. 5 and Tab. 6.

Table 4: Aircraft dynamic modes.

Mode	Pole	Damping	Frequency (rad/s)
Short Period	-5.32 $\pm$ j3.51	0.835	6.37
Phugoid	-0.0409 $\pm$ j0.303	0.134	0.306
Dutch Roll	-1.07 $\pm$ j4.27	0.242	4.40
Roll	-6.28	1	6.28
Spiral	-5.75e-3	1	5.75e-3

Feedback control system tunning

The determination of the gain matrix $\mathbf{K}$ for the proposed control systems requires the selection of the tuning matrices. The tuning matrices adopted for this analysis are shown in Tab. 7 and were manually defined by iterative adjustments.

Using the values of the linearized systems, presented in Tab. 5 and Tab. 6, and the tuning values, presented in Tab. 7, is possible to determine the gain matrix $\mathbf{K}$ for each system. In this work, the `lqr` algorithm available in Matlab was adopted to this task. Due the configuration of the system, the `lqr` outputs the value of the product $\mathbf{KC}$, as can be seen in Eq. (20). Then, the value of $\mathbf{K}$ can be determined, given that the $\mathbf{C}$ matrix is known. Thus, the resulting gain matrices obtained by the output-feedback LQR formulation, for the longitudinal and lateral-directional controllers, are shown in Tab. 8.

Table 5: State matrix and input matrix of the linearized longitudinal dynamics.

$$\mathbf{A}_{lo} = \begin{bmatrix} -0.1085 & -0.0138 & -0.0023 & -0.1712 & 0.0001 & 0 \\ -1.0327 & -2.3952 & 0.9705 & 0 & 0.0017 & 0 \\ 0 & -21.3461 & -8.2118 & 0 & 0 & 0 \\ 0 & 0 & 1.0000 & 0 & 0 & 0 \\ 0 & -0.5760 & 0 & 0.5760 & 0 & 0 \\ 0 & 0 & 0 & 0 & 0 & 0 \end{bmatrix} \quad \mathbf{B}_{lo} = \begin{bmatrix} 5.4571 & -0.0523 & 0 & 0 \\ 0.0402 & -0.6612 & 0 & 0 \\ 0 & -38.7019 & 0 & 0 \\ 0 & 0 & 0 & 0 \\ 0 & 0 & 0 & 0 \\ 0 & 0 & 0 & 0 \end{bmatrix}$$

Table 6: State matrix and input matrix of the linearized latero-directional dynamics.

$$\mathbf{A}_{ld} = \begin{bmatrix} -0.0743 & 0.2972 & -0.0029 & -1.0011 & 0 & 0 \\ 0 & -0.0000 & 1.0000 & -0.0042 & 0 & 0 \\ -16.7678 & 0 & -6.0798 & 2.2535 & 0 & 0 \\ 16.0196 & 0 & -1.0812 & -2.2643 & 0 & 0 \\ 0 & 0.0000 & 0 & 1.0000 & 0 & 0 \\ 0.5760 & 0.0024 & 0 & 0 & 0.5760 & 0 \end{bmatrix} \quad \mathbf{B}_{ld} = \begin{bmatrix} 0 & 0 & -0.0122 & 0.0057 \\ 0 & 0 & 0 & 0 \\ 0 & 0 & 39.3158 & -6.6444 \\ 0 & 0 & 4.0289 & 7.5661 \\ 0 & 0 & 0 & 0 \\ 0 & 0 & 0 & 0 \end{bmatrix}$$

Table 7: Tuning parameters used to calculate the LQR controller gain matrix.

$$\mathbf{Q}_{lo} = \begin{bmatrix} 200 & 0 & 0 & 0 & 0 & 0 \\ 0 & 150 & 0 & 0 & 0 & 0 \\ 0 & 0 & 1 & 0 & 0 & 0 \\ 0 & 0 & 0 & 1 & 0 & 0 \\ 0 & 0 & 0 & 0 & 1 & 0 \\ 0 & 0 & 0 & 0 & 0 & 0.0010 \end{bmatrix} \quad \mathbf{R}_{lo} = \begin{bmatrix} 1 & 0 & 0 & 0 \\ 0 & 0.5 & 0 & 0 \\ 0 & 0 & 1000 & 0 \\ 0 & 0 & 0 & 1000 \end{bmatrix}$$

$$\mathbf{Q}_{ld} = \begin{bmatrix} 0.1 & 0 & 0 & 0 & 0 & 0 \\ 0 & 10 & 0 & 0 & 0 & 0 \\ 0 & 0 & 1.5 & 0 & 0 & 0 \\ 0 & 0 & 0 & 1.2 & 0 & 0 \\ 0 & 0 & 0 & 0 & 1.3 & 0 \\ 0 & 0 & 0 & 0 & 0 & 0.1 \end{bmatrix} \quad \mathbf{R}_{ld} = \begin{bmatrix} 1000 & 0 & 0 & 0 \\ 0 & 1000 & 0 & 0 \\ 0 & 0 & 1 & 0 \\ 0 & 0 & 0 & 1 \end{bmatrix}$$

Table 8: Gain matrices obtained by the output-feedback LQR formulation.

$$\mathbf{K}_{lo} = \begin{bmatrix} 14.1522 & -1.3976 & 0.0070 & 0.9880 & 0.3664 \\ 0.0518 & -11.3942 & -1.3069 & -3.8653 & -1.3032 \\ 0.0000 & -0.0000 & -0.0000 & 0.0000 & 0.0000 \\ 0.0000 & 0.0000 & 0.0000 & 0.0000 & 0.0000 \end{bmatrix} \quad \mathbf{K}_{ld} = \begin{bmatrix} -0.0000 & -0.0000 & 0.0000 & 0.0000 \\ 0 & 0 & 0 & 0 \\ 3.3562 & 1.1273 & 0.1901 & 2.0832 \\ -0.5528 & -0.2410 & 0.8539 & 0.9845 \end{bmatrix}$$

RESULTS

This section presents the results obtained with the proposed feedback system, comparing the results obtained with the open-loop system with the closed-loop system. Keeping straight, wings-level, zero-sideslip, flight condition by applying the input $\mathbf{u}_{eq}$, which results in $\mathbf{x}_{eq}$, the system will be disturbed by deflecting the control surfaces and the thruster. The disturbance consist of a variation to the control inputs, applied as a rectangular pulse with duration of 1 second, which starts at 2 seconds of the simulation. The control surfaces is shifted by 10 degrees from the equilibrium point and the thruster is shifted to 100 %, as shown in Fig. 5.

An analysis of the open-loop response due to perturbations separetly applied to the longitudinal and lateral-directional dynamics are shown, respectively, in Fig. 6 and Fig. 7 which, together with the information available in Table 4, allow pointing out the characteristic of the underdamped response of the aircraft in both cases. It is also worth mentioning the

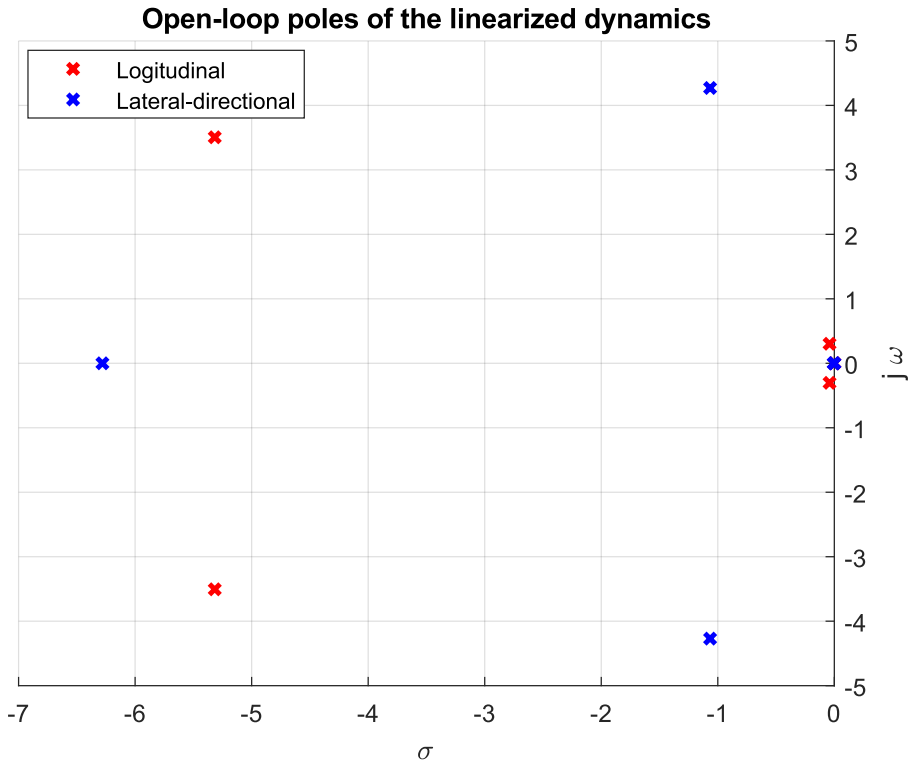

Figure 4: Open loop simulation Vector-P.

low damping factor of both scenarios, justifying the insertion of the SAS to control this undesired behavior.

The closed-loop feedback poles can be computed by the analysis of the eigenvalues of equivalent state matrix of the feedback system: $(\mathbf{A} - \mathbf{BKC})$, as can be inspected in Eq. (20), and the closed-loop poles are presented in Tab. 9 and Tab. 10.

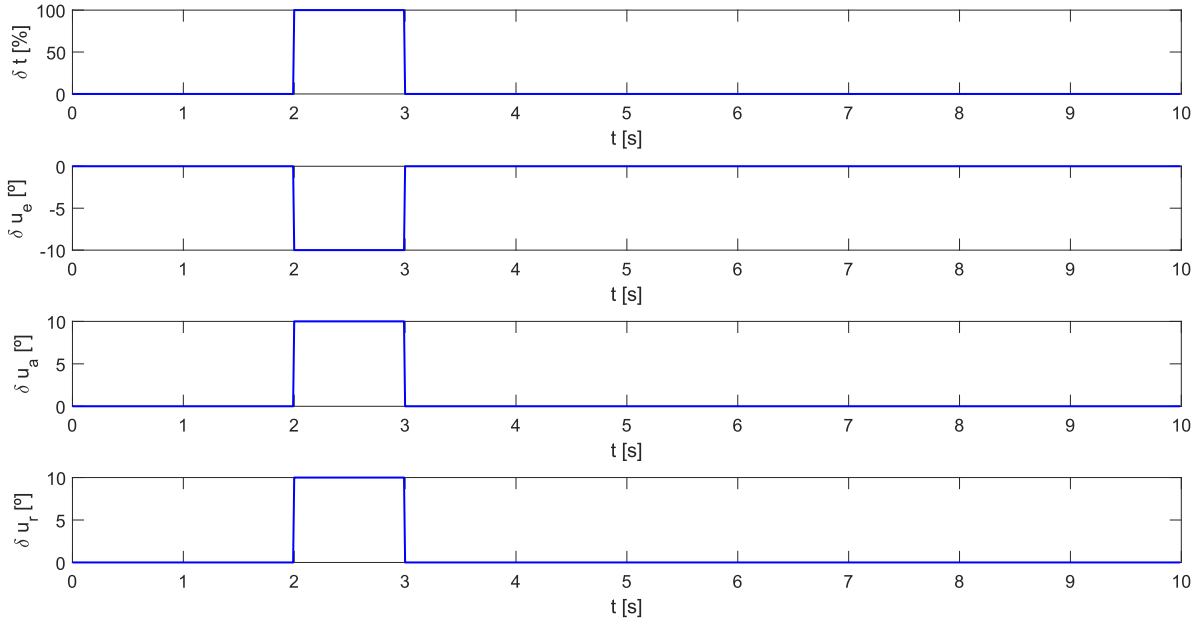

Figure 5: Representation of the disturbances ($\delta\mathbf{u}$) added to the aircraft's control inputs ($\mathbf{u}$).

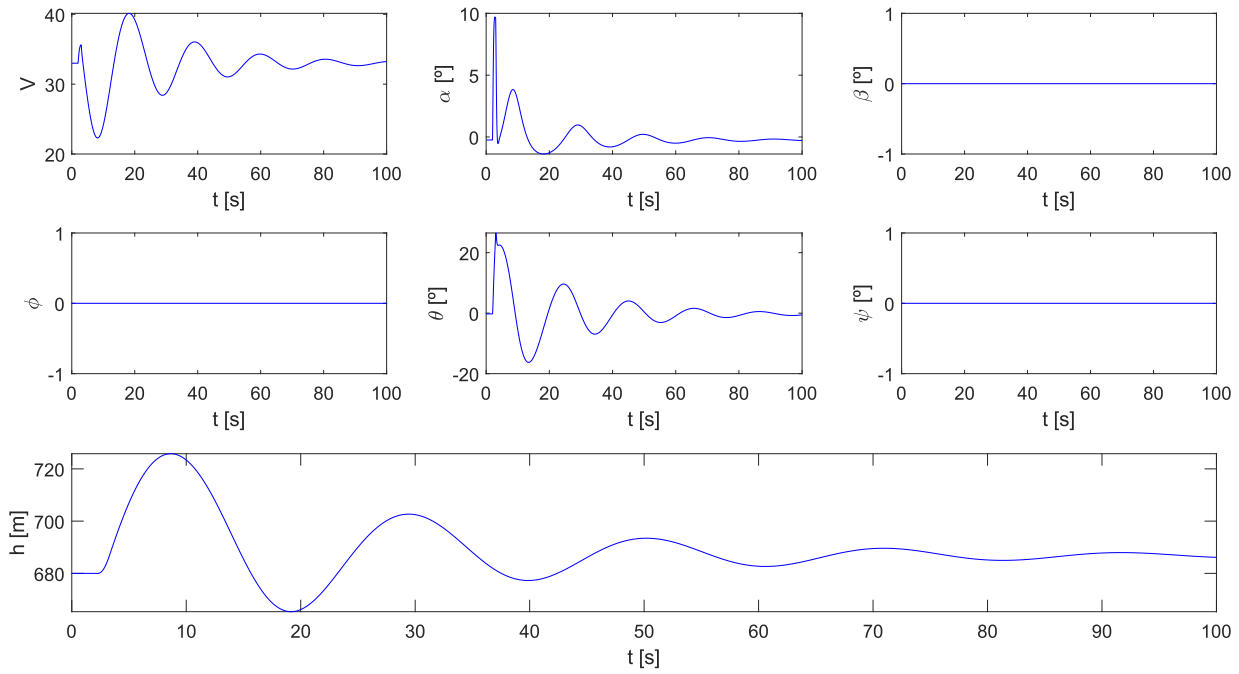

Figure 6: Open-loop response ($\mathbf{x}$) due to a disturbance in the longitudinal dynamics ($\delta\mathbf{u} = [\delta_t \ \delta_e \ 0 \ 0]^{\mathrm{T}}$) .

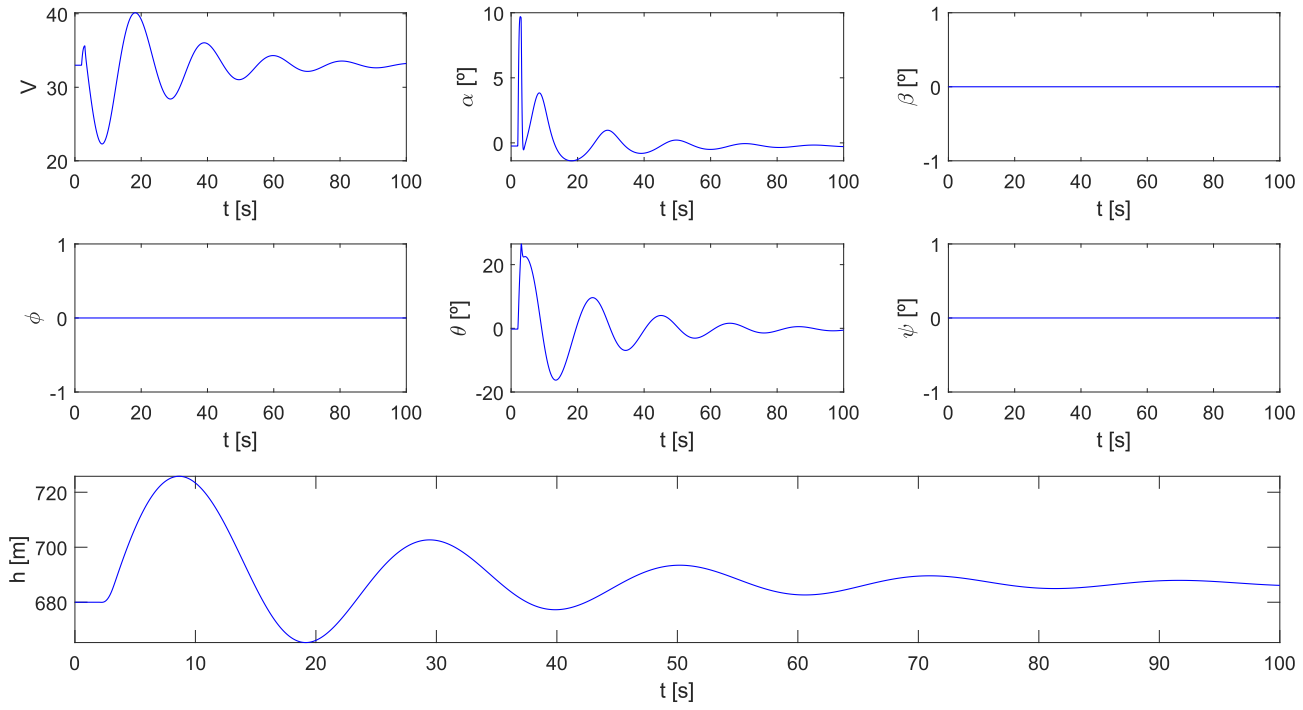

Figure 7: Open-loop response ($\mathbf{x}$) due to a disturbance in the latero-directional dynamics ($\delta\mathbf{u} = [0 \ 0 \ \delta_a \ \delta_r]^{\mathrm{T}}$) .

Logintudinal controller response

Table 9: Aircraft longitudinal dynamic modes with feedback control.

Pole	Damping	Frequency (rad/s)
-77.2	1.00	77.2
-54.4	1.00	54.4
-13.9	1.00	13.9
-0.229 $\pm$ j0.20	0.752	0.304
-0.00205	1.00	0.00205

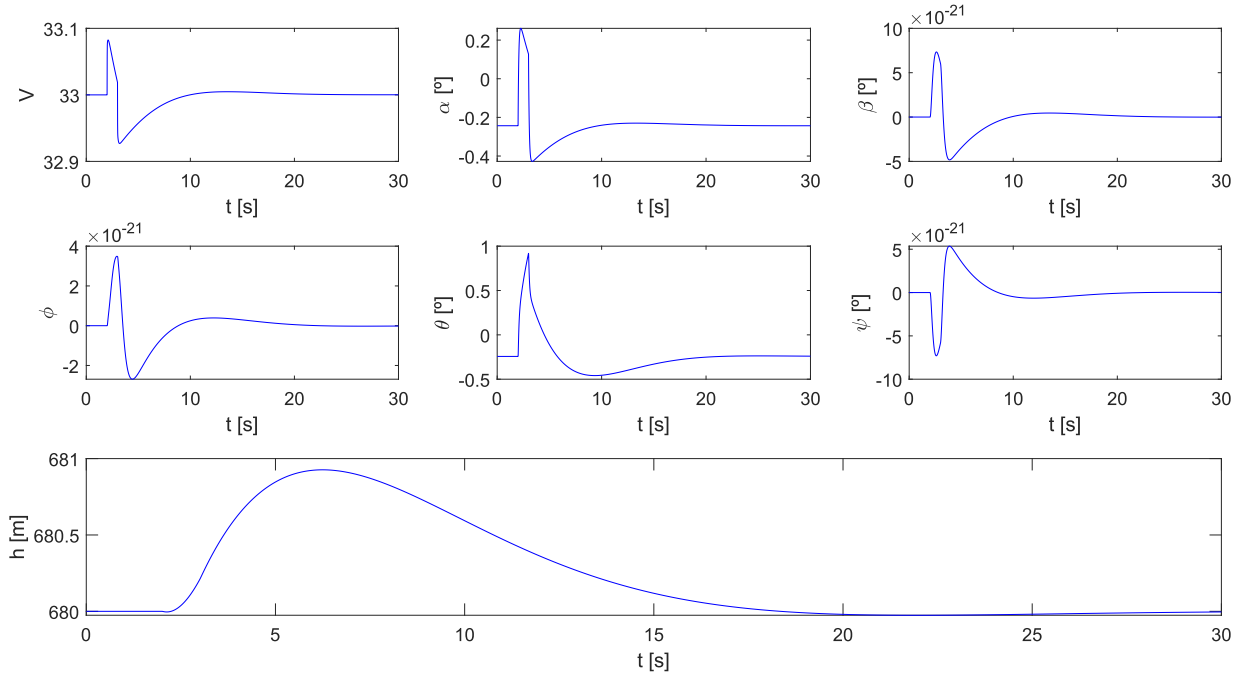

(a) $\mathbf{x}(t)$ response.

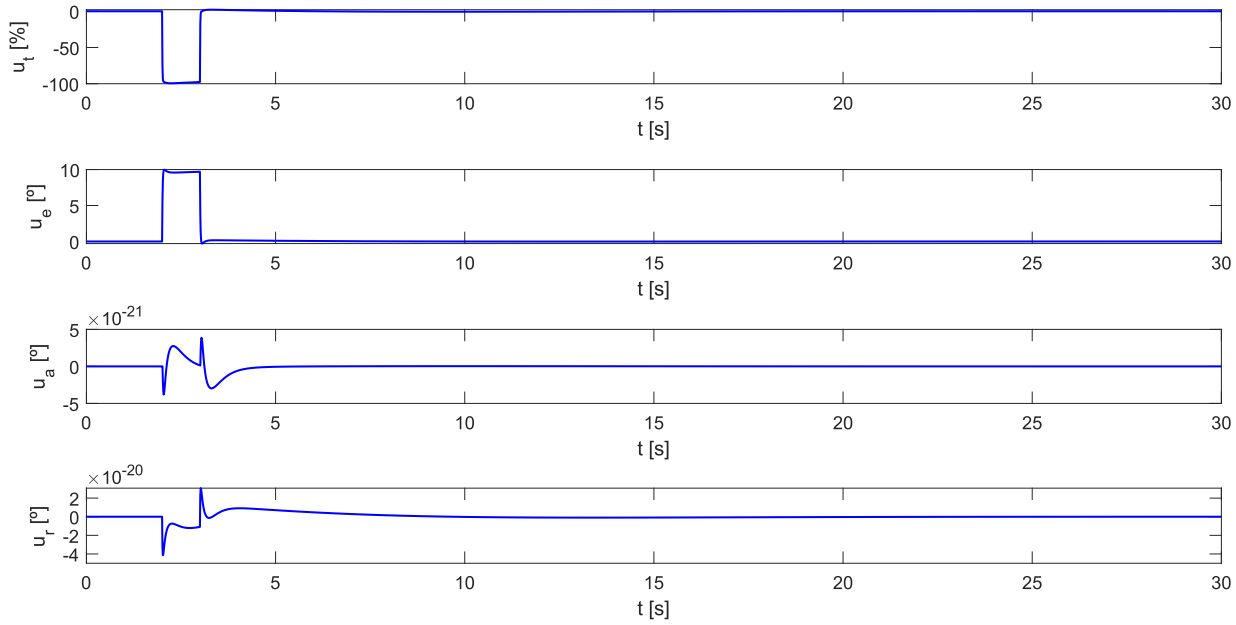

(b) $\mathbf{u}(t)$ response.

Figure 8: Closed-loop response ($\mathbf{x}$) due to a disturbance in the longitudinal dynamics ($\delta\mathbf{u} = [\delta_t \ \delta_e \ 0 \ 0]^{\mathrm{T}}$).

Latero-directional controller response

Table 10: Aircraft latero-directional dynamic modes with feedback control.

Pole	Damping	Frequency (rad/s)
-92.2	1.00	92.2
-6.4	1.00	6.4
-0.108 $\pm$ *j*0.0803	0.0802	9.28
-3.15	1.00	3.15
-2.05	1.00	2.56

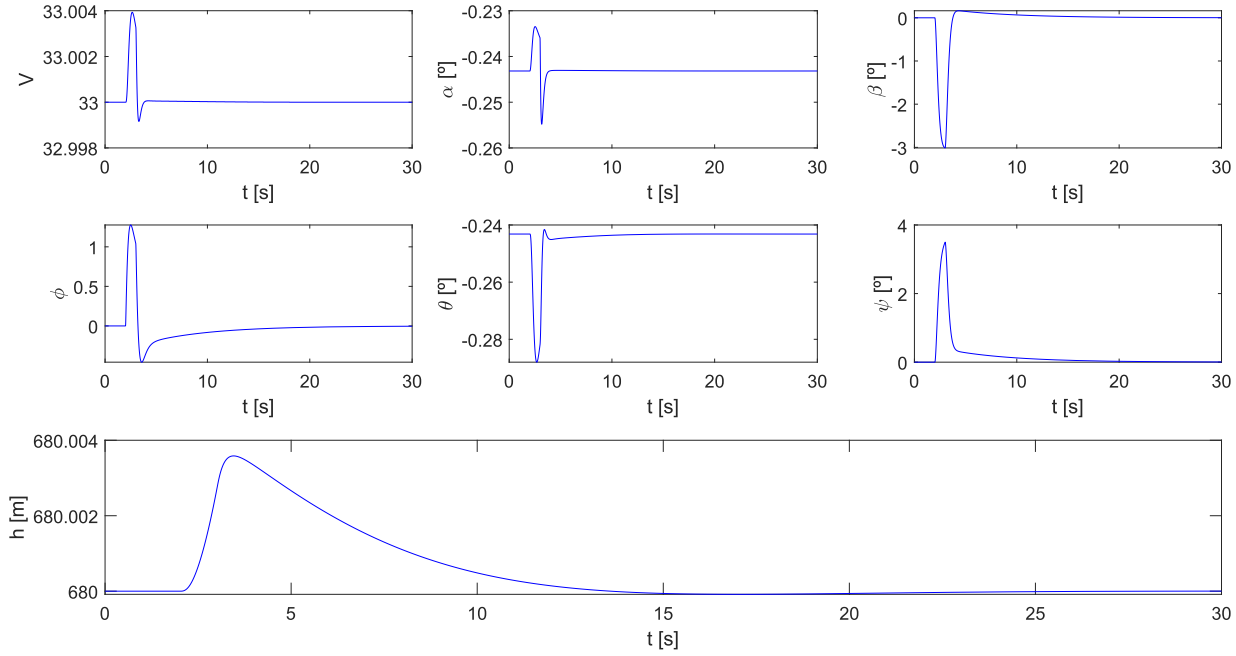

(a) $\mathbf{x}(t)$ response.

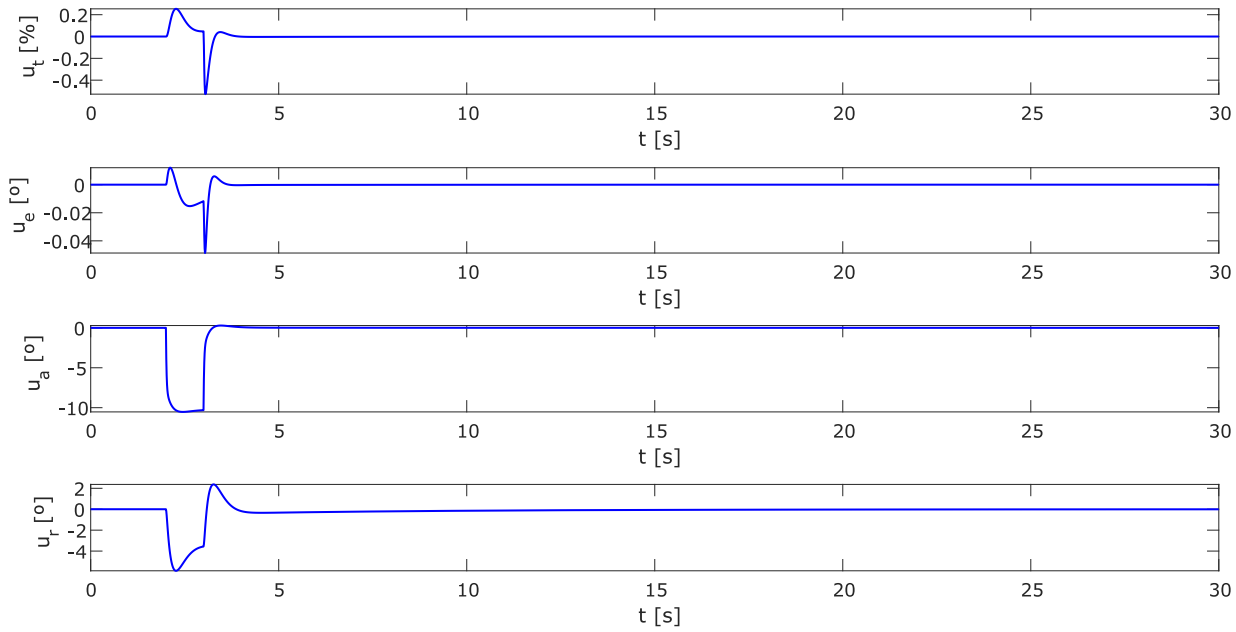

(b) $\mathbf{u}(t)$ response.

Figure 9: Closed-loop response ($\mathbf{x}$) due to a disturbance in the latero-directional dynamics ($\delta\mathbf{u} = [0\ 0\ \delta_a\ \delta_r]^{\mathrm{T}}$).

Combined response and analysis

Table 9 and Tab. 10 present the change in the characteristic of closed-loop poles when compared with the behavior in open-loo, see Tab. 4. It is possible to notice that the poles of the feedback system eliminated most of the oscillatory characteristic, in addition to presenting a fast speed response. This characteristic can also be seen with the graphs with the temporal response, presented in Figure 8 for the longitudinal control and in Figure 9 for the latero-directional control. For an analysis of the conjugated actuation of both control systems, a simulation was performed considering the insertion of disturbances in the four control inputs, see Fig. 5. The result to this situation is shown in Fig. 10. This demonstrates that the proposed control system is able to recover the desired configuration for the state variables, even with multiple external disturbance factors.

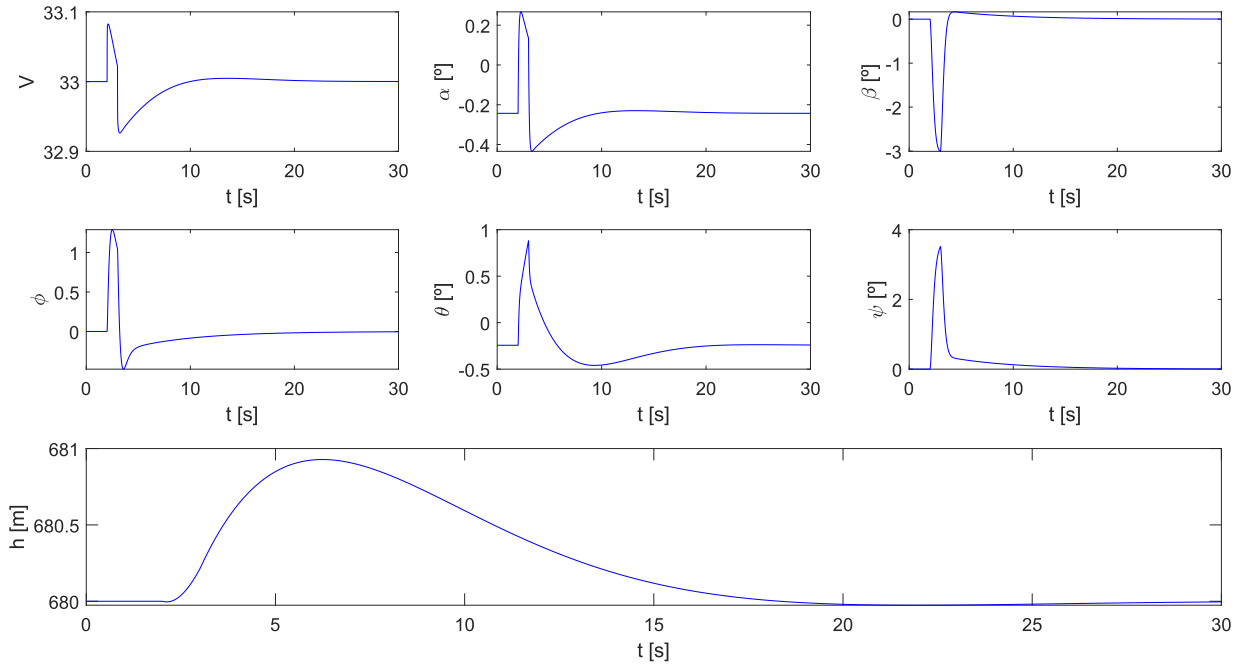

(a) $\mathbf{x}(t)$ response.

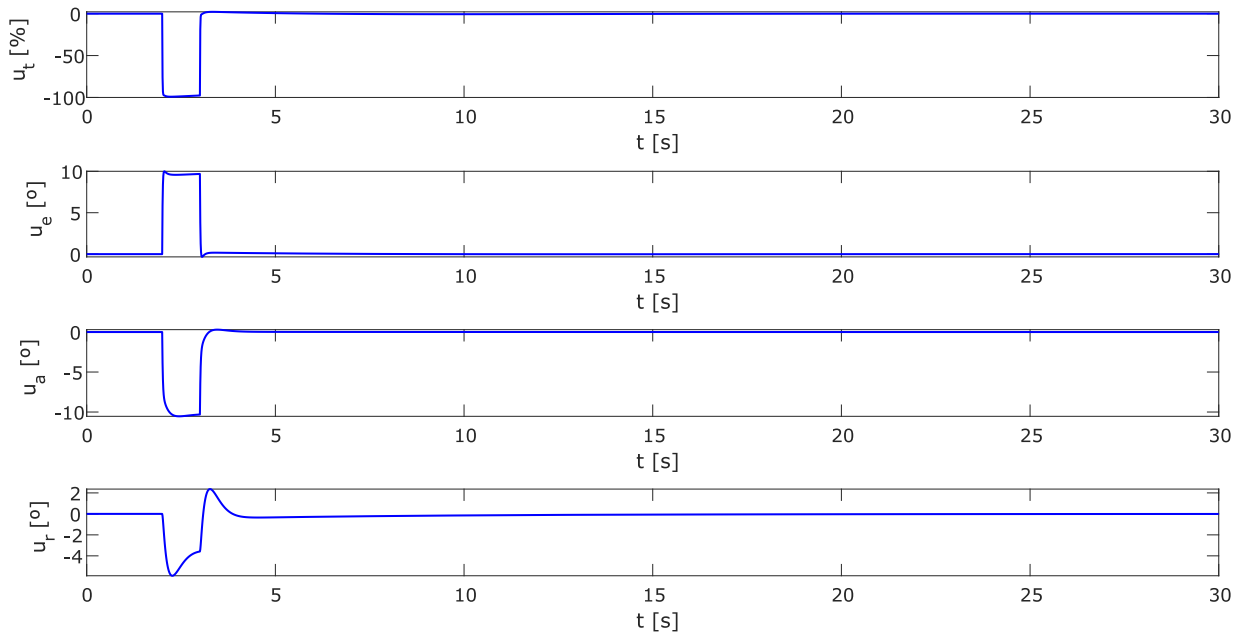

(b) $\mathbf{u}(t)$ response.

Figure 10: Closed-loop response ($\mathbf{x}$) due to a disturbance in the both longitudinal and latero-directional dynamics ($\delta\mathbf{u} = [\delta_t\ \delta_e\ \delta_a\ \delta_r]^{\mathrm{T}}$).

In this case, the system responses to disturbance show how the LQR controllers act effectively for the Autopilot/SAS

functions that they were designed for. By changing the closed-loop poles location, the SAS changes the aircraft dynamical modes, suppressing the oscillatory behavior, which reduces the risk of loss of control in flight. Likewise, the autopilot ensures that certain flight criteria are guaranteed, even in the presence of external disturbances. In this way, the system proved to meet the operational requirements initially proposed.

CONCLUSION

This work was motivated by the use of the UAV Vector-P in the research activities of the LSA-ITA, where its use can be in autonomous or remotely-piloted navigation activities. Throughout these studies, the need to design a control system for the Autopilot/SAS functions was identified. For this purpose, this work adopted the formulation of the output-feedback LQR, designed with the Vector-P identified model. In order to understand the procedures involved in the LQR design, the work presented the stages of development of the control laws and the details of the calculation methods, necessary to obtain the gain matrices. In addition, an analysis of the dynamic behavior of the system with and without the control loop was presented.

In the simulation it can be seen that the performance of the controllers will improve the dynamics of the aircraft as well as being able to follow the references and the flight conditions that were imposed.

For future works, it is intended to explore other aspects of the flight control system, evaluating the insertion of an autonomous navigation capability, so that the aircraft is able to follow pre-defined trajectories, as well as carrying out experimental evaluations of the presented proposal.

REFERENCES

Barbosa, R.C.M.G., Góes, L.C.S., Nabarrete, A., Balthazar, J.M. and Zúñiga, D.F.C., 2019. "Nonlinear identification using polynomial narmax model and a stability analysis of an aeroelastic system". In A.d.T. Fleury, D.A. Rade and P.R.G. Kurka, eds., *Proceedings of DINAME 2017*. Springer International Publishing, Cham, pp. 97–109. ISBN 978-3-319-91217-2.

Etkin, B. and Reid, L.D., 1995. *Dynamics of flight, stability and control*. John Wiley, Toronto.

Fischer, C., Nepomuceno, L.M., Silva, R.G.A.D. and Góes, L.C.S., 2018. "Identification of the lateral-directional model of the vector-p, unmanned aerial vehicle". In *31st Congress of the International Council of the Aeronautical Sciences, ICAS*. Belo Horizonte, MG, Brazil.

Nelson, R.C., 1989. *Flight stability and automatic control*. MCGraw-Hill, New York.

Santos, J.S., 2013. *IDENTIFICAÇÃO E CONTROLE DE UM VEÍCULO AÉREO NÃO TRIPULADO: VECTOR-P (in Portuguese)*. Master's thesis, Curso de Engenharia Aeronáutica e Mecânica, Área de Mecânica e Controle do Voo – Instituto Tecnológico de Aeronáutica, São José dos Campos, Brasil.

Stevens, B.L. and Lewis, F.L., 1992. *Aircraft control and simulation*. John Wiley and Sons.

RESPONSIBILITY NOTICE

The authors are the only responsible for the printed material included in this paper.